A flock-like two-dimensional cooperative vehicle formation model based on potential functions

Hao, Ruochen; Liu, Meiqi; Ma, Wanjing; van Arem, Bart; Wang, Meng

DOI
10.1080/21680566.2022.2052998

Publication date
2022

Document Version
Final published version

Published in
Transportmetrica B

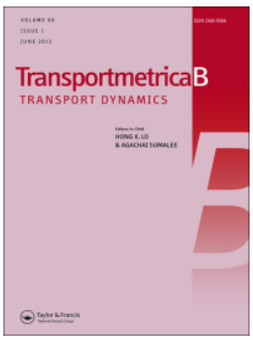

Transportmetrica B: Transport Dynamics

ISSN: (Print) (Online) Journal homepage: https://www.tandfonline.com/loi/ttrb20

A flock-like two-dimensional cooperative vehicle formation model based on potential functions

Ruochen Hao, Meiqi Liu, Wanjing Ma, Bart van Arem & Meng Wang

To cite this article: Ruochen Hao, Meiqi Liu, Wanjing Ma, Bart van Arem & Meng Wang (2022): A flock-like two-dimensional cooperative vehicle formation model based on potential functions, Transportmetrica B: Transport Dynamics, DOI: 10.1080/21680566.2022.2052998

To link to this article: https://doi.org/10.1080/21680566.2022.2052998

Published online: 13 Apr 2022.

TRANSPORTMETRICA B: TRANSPORT DYNAMICS
https://doi.org/10.1080/21680566.2022.2052998

Taylor & Francis
Taylor & Francis Group

A flock-like two-dimensional cooperative vehicle formation model based on potential functions

Ruochen Hao[a,b], Meiqi Liu[a], Wanjing Ma [b], Bart van Arem [a] and Meng Wang[a,c]

[a]Department of Transport & Planning, Delft University of Technology, Delft, The Netherlands; [b]Key Laboratory of Road and Traffic Engineering of the Ministry of Education, Tongji University, Shanghai, People's Republic of China; [c]Chair of Traffic Process Automation, Technische Universität Dresden, Dresden, Germany

ABSTRACT

Due to the manoeuvre complexity, models describing the platoon formation process on urban roads are lacking in the literature. Inspired by flocking behaviours in nature, we proposed a two-dimensional model to describe connected automated vehicle (CAV) group dynamics based on the potential theory, which is composed of the elastic potential energy for the inter-vehicle spring-mass system and the cross-section artificial potential field. The inter-vehicle elastic potential energy enables CAVs to attract each other at long distances, and repel each other otherwise. It also generates incentives for lane changes. The cross-section artificial potential field is able to mimic the lane-keeping behaviour and creates resistance to avoid unnecessary lane changes at very low incentives. These modelling principles can also be applied to human-driven vehicles in a mixed traffic environment. The behavioural plausibility of the model is demonstrated analytically and further verified in a simulation of typical driving scenarios.

ARTICLE HISTORY
Received 11 March 2021
Accepted 10 March 2022

KEYWORDS
Platoon management; connected and automated vehicle; platoon formation; microscopic model

1. Introduction

Connected and automated vehicles (CAVs) have the potential to affect the traffic flow characteristics and traffic management and control (Pei et al. 2019). Unlike individual automated vehicles which rely solely on on-board sensors, CAVs have advantages in both situation awareness and cooperative manoeuvring (Wang et al. 2014). As one of the earliest CAV applications, platooning has attracted a lot of attention due to the underlying benefits of improving roadway capacity and energy economy. Earlier studies in Intelligent Vehicle Highway System (IVHS) demonstrated that highway capacity can be improved by applying platooning (Tan, Rajamani, and Zhang 1998).

The architecture of IVHS is composed of the network layer, link (traffic control) layer, the platoon planning/management layer, the platoon/vehicle control layer, and the physical layer (Baskar et al. 2011). The platoon management layer deals with manoeuvre strategies of platoon formation, merge, split, dissolution, in addition to platoon member selection (Jia et al. 2015; Shladover et al. 2016; Zhan et al. 2021). On the contrary, the platoon control layer focuses on motion control, which transfers management strategies to executable trajectories. Existing studies focused on platoon control layer, resulting in significant contributions on string-stable platooning controller design (Shladover et al. 2016; Jia, Ngoduy, and Vu 2019; Sau, Monteil, and Bouroche 2019), with advances in dealing with

CONTACT Meng Wang m.wang@tudelft.nl, meng.wang@tu-dresden.de Department of Transport & Planning, Delft University of Technology, 2628 CN, Delft, The Netherlands; Chair of Traffic Control and Process Automation, Technische Universität Dresden, 01069, Dresden, Germany; Wanjing Ma mawangjing@tongji.edu.cn Key Laboratory of Road and Traffic Engineering of the Ministry of Education, Tongji University, 4800 Cao'an Road, Shanghai, People's Republic of China

delays (Zhang et al. 2020; Jin and Orosz 2016), uncertainties (Chen et al. 2018), and the heterogeneous platoon (Wang et al. 2014). For extensive review of the control architectures, the control methods and string stability analysis of the platoon control layer, we refer to Wang, Wu, and Barth (2018).

Modelling and control design at the platoon management layer receives much less attention compared with the platoon control layer. Active route planning strategies for platoon formation focused on optimizing routing and departure time to increase the chance of CAVs meeting each other along their routes (Turri, Besselink, and Johansson 2016; Van de Hoef 2016). But the operational processes to form the platoon are not considered. Although platoon operations can be interrupted by intersections on urban roads, forming platoons can still be favourable since it not only improves the throughput of the road network but also reduces the complexity of the traffic control layer, i.e. the platoon of several vehicles can be treated as one control unit. There are a number of studies optimizing platoon trajectories at signalized intersections assuming that vehicles already form platoons when entering the network (Han, Ma, and Zhang 2020; Chen et al. 2015). The research summarized in Rios-Torres and Malikopoulos (2016) excludes the platoon formation under the urban environment.

Limited studies consider the active platoon management strategies at signalized intersections. Existing research efforts on platoon formation are rule-based, according to the signal timing (Faraj, Sancar, and Fidan 2017) or the communication range (Jin et al. 2013). Tallapragada and Cortés (2017) uses K-mean clustering to form platoons in order to ensure the size of formed platoons is similar to the requirement of the intersection traffic controller. The decentralized control is proved to be economical (Otto and Bustamante 2009). The decentralized control reported by Hallé, Laumonier, and Chaib-Draa (2004) focuses on the process of merging and splitting, but did not consider traffic signal control. Moreover, the mixed traffic environment is ignored. Yao, Shet, and Friedrich (2020) proposes a decentralized platoon strategy based on the maximal platoon size on urban roads under the mixed traffic environment. However, the lateral lane change behaviour is not considered.

Swarm intelligence is an important decentralized control method that has been widely used in unmanned aerial vehicles (UAVs) related research. Swarm intelligence control is a control method that allows the overall group to reach the desired target by setting local interaction rules for each agent according to several principles. Swarm intelligence can be used for both platoon formation and tracking (Ren and Cao 2010). With respect to formation, the matrix-based approach and the Lyapunov-based approach are included (Cao et al. 2012). As for formation tracking, the behaviour-based approach and the potential field approach have been used (Das, Subudhi, and Pati 2016). Swarm intelligence models originate from the basic flock principles proposed by Reynolds (1987) in 1987. Existing flock-like models for UAVs mainly focus on selecting the platoon leader and building communication network (Cooper et al. 2016), while neglecting the potential system and detailed motions. Artificial potential fields were applied in recent studies to control motions of multi-vehicles (Yi et al. 2020),especially under the mixed traffic (Kanagaraj and Treiber 2018). Li et al. (2017) applied the spring-mass system theory to establish the car-following model based on the elastic potential field, and Li et al. (2019) considered time delay and stability analysis in the spring-mass-damper-clutch system. Bang and Ahn (2017) used swarm intelligence as the control strategy and spring-mass-damper system theory as agent interaction rules. But these are limited to longitudinal vehicle motion. Since the dynamic characteristics of on-road vehicles are different from the UAVs or other common research objects of swarm intelligent, existing potential system of swarm intelligence cannot be used directly to two-dimensional cooperative vehicle group dynamics.

To summarize, although numerous efforts on platooning have been made, there are still some scientific gaps on platoon management and control at urban networks. Platoon formation is usually considered as a centralized macroscopic level problem (Luo, Larson, and Munson 2018), which plans vehicle routes and schedules to form platoons but ignores the detailed formation processes. Existing microscopic approaches do not fully utilize the flock-like model, so vehicles are operated in one dimension with a myopic horizon. As a result, limited studies consider the vehicle sequence adjustment (Tallapragada and Cortés 2017), especially in the urban environment. Owing to different turnings and routing choices of CAVs, the orders of CAVs are critical in the traffic control (i.e. adaption of signals

based on the class-specific traffic demand levels can achieve better traffic control performance). Additionally, most platoon formation methods can only work in a fully CAV environment, and the influence of human-driven vehicles (HVs) is ignored in many studies.

This paper proposed a flock-like vehicular behaviour model with flexible formation in two dimensions. This model integrates the tactical manoeuvre with the operational motion dynamics using the combined potential-based formation. Existing potential functions are usually used for modelling longitudinal interactions between consecutive vehicles, such as the spring-mass system (Li et al. 2019). These functions fail to unify the potential force among multiple vehicles and in the cross-section of the road. To fill this scientific gap, this paper introduces the cross-section potential force, in addition to the potential force among vehicles. The proposed model can incorporate two dimensions of longitudinal and lateral motions directly. Furthermore, lane allocation is also considered in the potential function. Vehicles can form platoons according to the requirements from the traffic control layer or based on vehicle classes using the attraction strength in the potential fields. The lane changing and the car following behaviours are considered, and the endogenous flocking principles of attraction (or flock centring), alignment (or velocity matching), and collision avoidance are captured in this model. Furthermore, this model can represent both CAVs and human-driven vehicles.

The remainder of this paper is organized as follows. Section 2 describes the problem and presents the platoon management model. The design of potential field is located in this section. Section 3 analyses the model mathematical properties. Section 4 uses some numerical studies to evaluate the performance of the proposed flock-like model and explore the reasonable ranges of parameters. Finally, conclusions and recommendations are provided in Section 5.

2. Model formulation

2.1. Problem description

The purpose of the proposed model is to describe the operation process of the formation of CAV platoons under the mixed traffic environment. Figure 1 illustrates the context of this study, which is a full intersection with a CAV exclusive lane, a left-turn lane and a through/right-turn lane in each approach. The intersection is divided into three zones, i.e. the staging zone, the adjusting zone and the centralized control zone. The centralized traffic controller collects CAV information in the staging zone and provides CAVs with the desired platoon formation information such as the platoon size and the CAV sequence. CAVs in the adjusting zone will change their positions and velocities to track the commands of desired formation from the traffic control layer. After platoons enter the centralized control zone, the centralized traffic controller will give the control instructions to the CAVs directly. The control structure is shown as Figure 2.

The focus of this paper is the platoon management layer in the adjusting zone. The proposed model describes the dynamic motions of both longitudinal and lateral dimensions to form the desired platoon formation in the adjusting zone, which is located at the platoon management layer. Shown as an example in Figure 1, four CAVs (i.e. ω_1, ω_2, ω_3 and ω_4) are in the staging zone. The centralized traffic controller requires ω_2, ω_3 and ω_4 to form a platoon on the CAV exclusive lane, and consequently these CAVs adjust the longitudinal and lateral motions in the adjusting zone for this common purpose.

2.2. Modelling principles based on flocking

The basic flocking model is proposed in Reynolds (1987). The model is composed of three principles: collision avoidance, velocity matching, and flock centring. Collision avoidance guarantees collision-free with other flockmates, and flock centring ensures that each flock member keeps close to the neighbouring flockmates and approaches to the perceived centre. Velocity matching aims to keep the same velocity of the neighbouring flockmates.

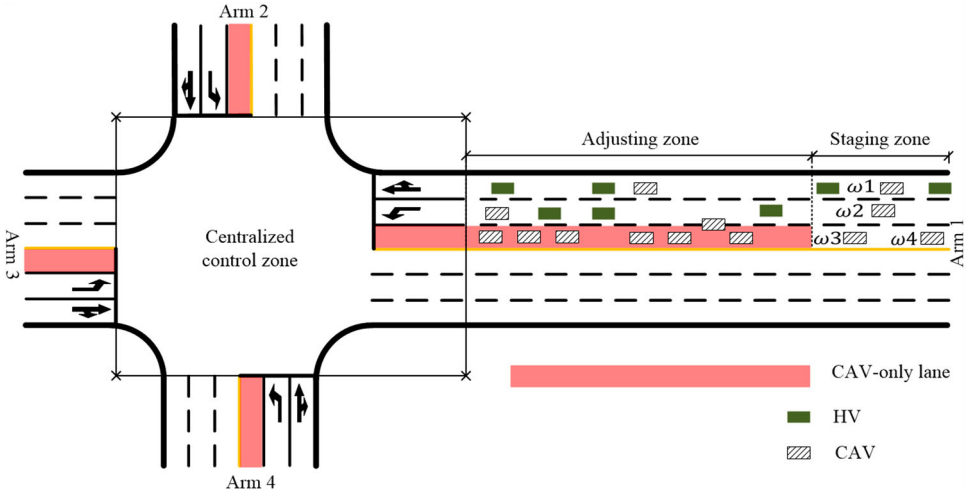

Figure 1. Intersection description.

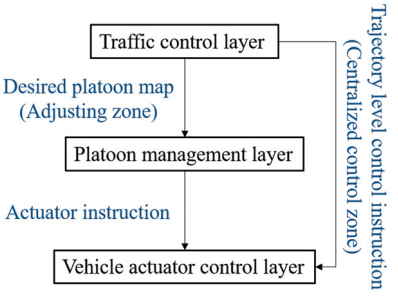

Figure 2. Intersection control structure.

Analogously, collision avoidance is one of the necessary requirements for CAVs. The velocity matching and flock centring behaviours are similar to the platoon stability in longitudinal direction as CAVs in the same group/formation aim to keep the same velocity and space headway. Therefore, the flock-like model is suitable to describe the platoon operations. In the remainder of this section, we will introduce the vehicle dynamics and constraints, as well as the mathematical specifications of these flocking principles.

2.3. Vehicle dynamics and constraints

The two-dimensional vehicle motion follows the basic kinematics law at a point mass. Let vector $\mathbf{x}_j$ denote the system state of vehicle j, which consists of the longitudinal and lateral positions (x_j and y_j), as well as the longitudinal and lateral velocities ($v_{x,j}$ and $v_{y,j}$).

$$\mathbf{x}_j = (x_j, v_{x,j}, y_j, v_{y,j})^{\mathsf{T}}, \tag{1}$$

where x is the longitudinal position in the driving direction along the road, and y is the lateral position on the direction perpendicular to the road. The state dynamics follows the second-order kinematic

equation as:

$$\begin{pmatrix} \dot{x}_j \\ \dot{v}_{x,j} \\ \dot{y}_j \\ \dot{v}_{y,j} \end{pmatrix} = \begin{pmatrix} v_{x,j} \\ a_{x,j} \\ v_{y,j} \\ a_{y,j} \end{pmatrix}, \tag{2}$$

where the longitudinal and lateral accelerations ($a_{x,j}$ and $a_{y,j}$) are model inputs. v_x, a_x and v_y, a_y are the velocity and acceleration on the longitudinal direction and the lateral direction, respectively.

In the two-dimensional vehicle kinematic model, acceleration and velocity are constrained to respect the realistic vehicle dynamics, including:

$$a_x^{\min} \leq a_{x,j} \leq a_x^{\max}, \tag{3a}$$

$$a_y^{\min} \leq a_{y,j} \leq a_y^{\max}, \tag{3b}$$

$$v_x^{\min} \leq v_{x,j} \leq v_x^{\max}, \tag{3c}$$

$$v_y^{\min} \leq v_{y,j} \leq v_y^{\max}. \tag{3d}$$

The velocity and acceleration limits are usually bounded within constant values. $a_x^{\min}, a_y^{\min}$ and $a_x^{\max}, a_y^{\max}$ are minimum and maximum longitudinal or lateral accelerations, respectively. Similarly, $v_x^{\min}, v_y^{\min}$ and $v_x^{\max}, v_y^{\max}$ are minimum and maximum longitudinal or lateral velocities, respectively. These parameters are determined by vehicle dynamics and road condition.

2.4. Vehicle formation model specification

It is assumed that CAVs perceive the states of other CAVs and HVs accurately in the perception range of their sensors and V2X devices, and the vehicle actuation systems in the lower level can precisely execute the control commands from the on-board controller. The 'mass' of vehicles in this study is set to the unit mass, which means the unit of force is m/s^2, i.e. the value of the lateral/longitudinal acceleration is equal to the value of the lateral/longitudinal force. Forces imposed on vehicles stem from interactions with surrounding vehicles and the deviation from the lane centre. These forces are considered as Potential Based Force (indicated by F).

The motion of a vehicle will be influenced by $p_{x,ij}^b, p_{y,ij}^b, p_j^c, p_j^d$, and p_j^f. $p_{x,ij}^b$ and $p_{y,ij}^b$ are the longitudinal and lateral inter-vehicle forces imposed on vehicle j caused by vehicle i. The cross-section force, p_j^c, constrains the vehicle j in the lateral dimension. Each CAV calculates $p_{x,ij}^b$ and $p_{y,ij}^b$ for all surrounding human-driven vehicles in the perception range of on-board sensors and other CAVs with the same platoon number within the communication range. CAVs with the same platoon number implies that the central traffic controller asks them to form a platoon, while the vehicle class can be used in the absence of a central traffic controller. Vehicles with the same vehicle class number may imply they have the same destination, target velocity or other features. HVs are assumed to estimate $p_{x,ij}^b$ and $p_{y,ij}^b$ considering all vehicles in the perception range of the driver. $p_{x,ij}^b$ and p_j^c will be introduced in detail in Sections 2.4.1 and 2.4.2.

The force acted on a vehicle can be decomposed into two perpendicular vectors, F_x and F_y, corresponding to the model inputs a_x and a_y in order to update the motion of the subject vehicle.

Let $\mathcal{N}$ and N denote the set of vehicles in the perception range of vehicle j, and the total number of vehicles in $\mathcal{N}$. In the longitudinal direction, $p_j^d(v_{x,j})$ and $p_{x,ij}^b(x_i, v_{x,i}, x_j, v_{x,j})$ act on vehicle j, thus the longitudinal force of vehicle j is

$$F_j^x = \sum_{i=1}^{N} p_{x,ij}^b(x_i, v_{x,i}, x_j, v_{x,j}) + p_j^d(v_{x,j}). \tag{4}$$

In the lateral dimension, the lateral force includes $p^b_{y,ij}(y_i, y_j)$, p^c_j, and p^f_j and thereby is calculated by

$$F^y_j = \sum_{i=1}^{N} p^b_{y,ij}(y_i, y_j) + p^c_j + p^f_j. \tag{5}$$

The accelerations of a^y_j and a^x_j can be calculated by force as Equations (6) and (7), where m is the mass of control unit. To simplify calculation, the mass is assumed as the unit mass. It is noted that the longitudinal and lateral forces are used to update the vehicle motions under the system dynamics Equation (2) and the motion constraints Equation (3a).

$$a^y_j = \frac{F^y_j}{m}, \tag{6}$$

$$a^x_j = \frac{F^x_j}{m}. \tag{7}$$

Force p^d_j is designed to operate the subject vehicle j in the desired velocity. If the value of p^d_j is set as the maximal acceleration, the vehicle j can accelerate to reach the desired velocity with the maximum acceleration providing no vehicles in front. The p^d_j is set as Equation (8):

$$p^d_j(v_{x,j}) = \max\left\{F_{\max}\left(\frac{v^{\max}_x - v_{x,j}}{v^{\max}_x}\right), 0\right\}. \tag{8}$$

In addition, a constant friction p^f_j is also considered to avoid the local oscillation of vehicles in the lateral dimension, which is perpendicular to the driving direction.

2.4.1. Inter-vehicle force

Inter-vehicle force guarantees that vehicles in a group attract each other but maintain at least the safe gap. The longitudinal inter-vehicle force is an elastic force. Its function is specified as follows:

$$p^b_{x,ij}(x_i, v_{x,i}, x_j, v_{x,j}) = c_{ij}\left(\ln(x_{ij}) - \frac{(x_e + t_c v_{x,j} - t_h \Delta v_{x,ij})\ln(x_e + t_c v_{x,j} - t_h \Delta v_{x,ij})}{x_{ij}}\right), \tag{9}$$

where x_e is the initial equilibrium distance in the longitudinal dimension. $x_{ij} = x_i - x_j$ is the longitudinal distance between vehicle i and vehicle j. $\Delta v_{x,ij} = v_{x,i} - v_{x,j}$ is the relative longitudinal velocity. c_{ij} is the attraction strength between the vehicle pair. For vehicles in the same group, the attraction strength between each vehicle pair are larger than the counterparts from different groups, leading to larger attractive forces to form a platoon. t_c is the constant time headway. t_h can be interpreted as desired time to collision. $p^b_{x,ij}$ in the longitudinal direction is calculated by the aforementioned parameters and variables.

The longitudinal inter-vehicle force function is shown in Figure 3, where t_h, c_{ij}, and x_e are set to 0.6 s, 1, and 3 m, respectively. Figure 4 shows how $p^b_{x,ij}$ changes with the velocity gap and the relative longitudinal distance, where t_h, c_{ij}, x_e are set as 0.6 s, 1, and 10 m, respectively. $p^b_{x,ij}$ is lower than 0 (i.e. the repulsive force) if the distance between vehicles is smaller than $x_e - t_h \Delta v_{x,ij}$, while the magnitude of $p^b_{x,ij}$ increases sharply with the decreases in distance between vehicles. This specification meets the *collision avoidance* principle from the safety perspective. When the velocity of the front vehicle is smaller than the velocity of the following vehicle, i.e. $\Delta v_{x,ij} < 0$ and $x_e - t_h \Delta v_{ij} > x_e$, the following vehicle is supposed to maintain a larger safety distance under this situation. In contrast, if the distance is larger than $x_e - t_h \Delta v_{x,ij}$, $p^b_{x,ij}$ (>0) increases slowly with the increases in distance and finally keeps the same velocity as the velocity of the front vehicle. As a result, vehicles tend to accelerate to reach the velocity of the front vehicle and maintain the gap of x_e, which satisfies the *velocity matching* and *flock centring* principles as well as the platooning requirements. Considering the domain of the potential function.

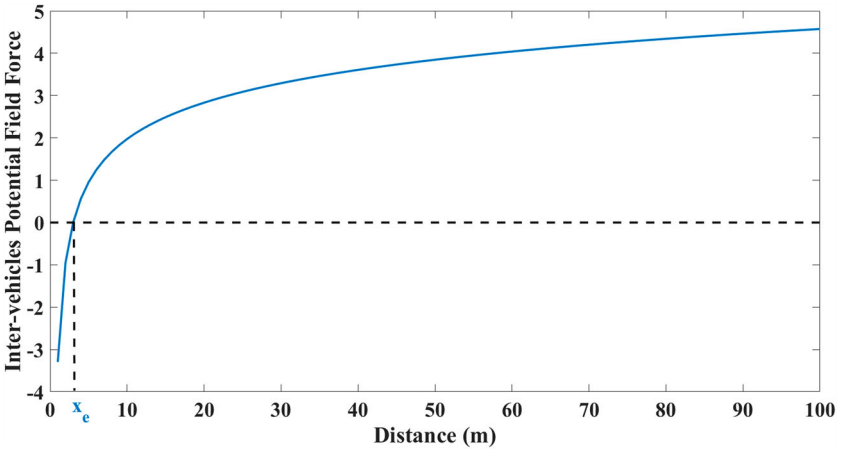

Figure 3. Inter-vehicle potential function.

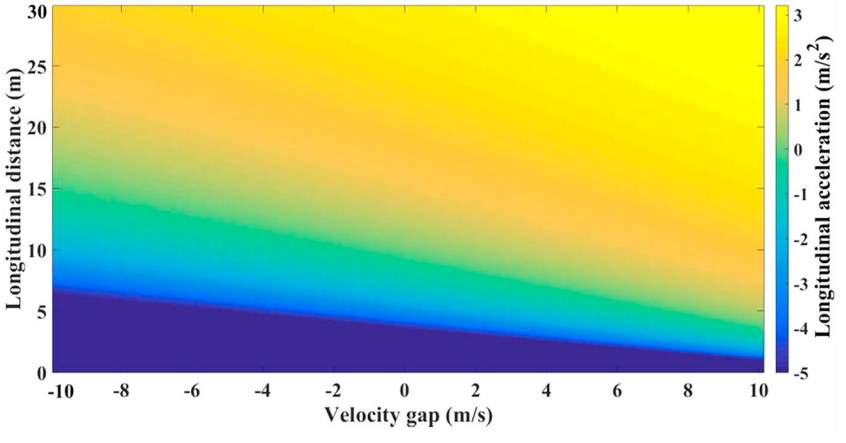

Figure 4. Longitudinal Inter-vehicle potential function force.

$x_e - t_h \Delta v_{x,j}(t)$ should be larger than 0. If it is not met, that means the velocity of the front vehicle is much larger than the following vehicle. The acceleration will be set as the largest allowed longitudinal acceleration.

As to estimating the lateral inter-vehicle force $p^b_{x,ij}(y_i, y_j)$, $x_e - t_h \Delta v_{x,ij}$ in (9) is replaced by $(y_e)_{ij}$, which is the constant lateral equilibrium distance. $(y_e)_{ij}$ is set as the lane width if vehicle i and vehicle j are in different platoons or the longitudinal distance between them is smaller than 5 m. Otherwise, $(y_e)_{ij} = 0$. The lateral inter-vehicle force function is specified as follows:

$$p^b_{y,ij}(y_i, y_j) = c_{ij}\left(\ln(y_{ij}) - \frac{(y_e)_{ij}\ln(y_e)_{ij}}{y_{ij}}\right). \tag{10}$$

To be noted, if the distances between vehicles equal to x_e and $(y_e)_{ij}$, respectively, and the vehicle pair has the same velocities $v_{x,i} = v_{x,j}$ (i.e. at equilibrium states), the inter-vehicle forces $p^b_{x,ij}$ and $p^b_{y,ij}$ equal to 0.

2.4.2. Cross-section artificial potential function

The cross-section artificial potential function is designed for the lane keeping and the lane changing behaviours. As for the lane-keeping behaviour, vehicles should stay within the lane and be motivated

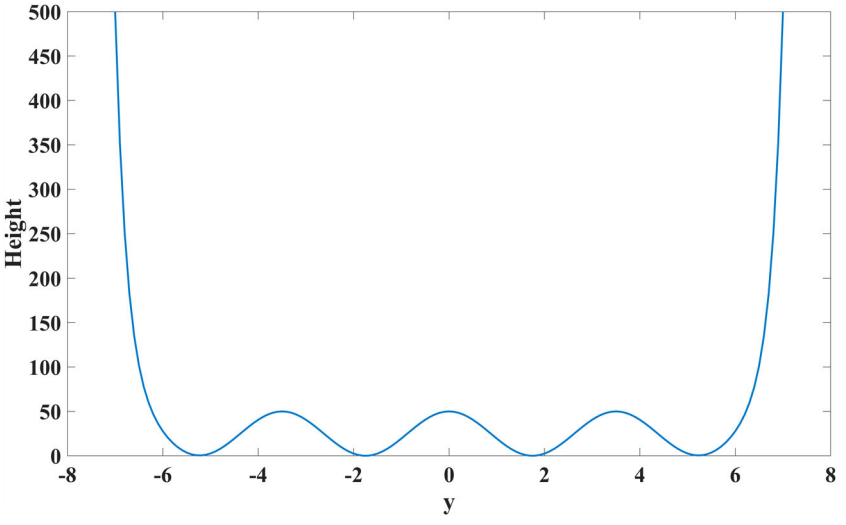

Figure 5. Cross-section artificial potential function at normal section.

to track the centre of its target lane. As a result, the cross-section artificial potential field is designed as a valley. The minimum and maximum values are set at the lane centre of the desired lane and at the boundaries of the road segment, respectively. The purpose of the maximum value H is to keep vehicles on the road.

As for the lane changing behaviour, vehicles should be stimulated to change lane by the inter-vehicle force $p^b_{y,ij}$. Vehicles are required to change lanes only when there is a vehicle in the same group but on another lane, i.e. exerting a large force to change lane. As a result, a small positive value h is set as the local maximum value at the lane boundaries instead of the global maximum value. Setting h can also prevent unnecessary lane changing behaviours.

According to the above design, the cross-section function is designed as Equation (11). The potential function is shown in Figure 5.

$$f(y) = \frac{h}{2}(1 - 2\,\mathrm{mod}(nl, 2))\cos\left(\frac{2y\pi}{w}\right) + \frac{h}{2} + (H - h)(\mathrm{e}^{\lambda(y - W/2)} + \mathrm{e}^{\lambda(-y - W/2)}), \tag{11}$$

where $W = nl * w$ is the road width, nl the number of lanes, w the lane width, λ the adjusted parameter. The cross-section force is calculated according to the cross-section potential function:

$$p^c_j = \frac{\partial f(y_j)}{\partial y_j}. \tag{12}$$

For road sections with lane allocations, the cross-section function is designed as follows. To define the cross-section artificial potential function(s), feature points and their heights are set. The cross-section artificial potential function and the feature points are demonstrated in Figure 6, taking the three-lane case as an example. The subfigures (a) to (c) represent the illustration of the potential field for lane allocation when the vehicle needs to change to the middle lane to pass the intersection, the artificial potential function when the vehicle enters the control zone, the artificial potential function when the vehicle is on the lane without the need of changing lanes, and the artificial potential function when the vehicle reaches the stop-line, respectively.

As shown in Figure 6(a), the feature points are characterized as two outer boundary points (marked yellow), two-lane boundary points (marked blue), and three-lane centre points (marked green). In Figure 6(c) to (b), the feature point height of the outer boundaries is always H ($= 500$), pushing the vehicle to stay in the boundary of three lanes, and the height of the lane centre at 0 m equals to 0 to trap

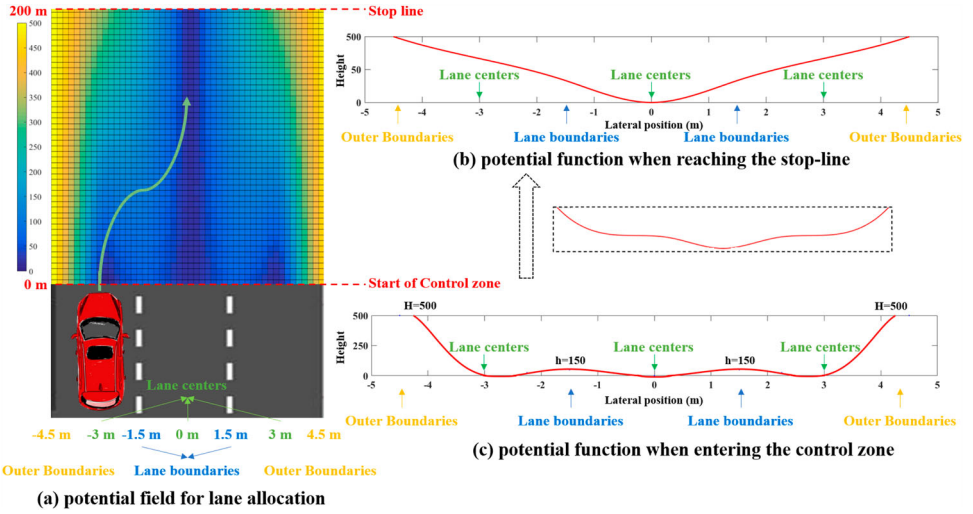

Figure 6. Cross-section artificial potential function at road section evolving lane allocations.

the vehicle in the middle lane. Other feature point heights vary gradually in Figure 6(c) to (b) to guide the vehicle to the target lane (as shown in Figure 6(a)). In other words, the cross-section artificial potential function will linearly change from Figure 6(c) to (b) from the moment when the vehicle reaches the control zone to the moment when the vehicle exits the intersection. During this process, the artificial potential field can be obtained by fitting the feature points with the Polynomial fit approach.

However, the cross-section artificial potential functions also have trouble when the vehicle is not at the lane centre and there are no other adjacent vehicles in the perception zone. In this situation, the lateral behaviour of the vehicle is controlled only by p_j^c, so the vehicle will oscillate in the valley if it deviates from the lane centre in the initial condition. To avoid this problem, a constant friction p_j^f is introduced, the direction of which is always opposite to the direction of the motion.

2.4.3. Additional rules for formation dynamics

Some additional rules are imposed to deal with the special situations. First, $p_{x,ij}^b$ and $p_{y,ij}^b$ between a CAV and other CAVs within the same platoon number or class should be different from $p_{x,ij}^b$ and $p_{y,ij}^b$ between a CAV and other vehicles. For instance, if two CAVs drive in parallel on different lanes of a road segment, they should change lane and form a platoon if they have the same platoon number or class, otherwise they should keep their current lanes. Additionally, the sequence of each CAV may be set by the centre controller. CAVs with the smaller sequence need to take over the CAVs with the larger sequence. For a specific CAV, if another CAV is behind it and the lateral distance between them is smaller than the half-width of the CAV exclusive lane, it is defined as a following CAV of the specific CAV. If a CAV detects that one of its following CAV has a smaller sequence, a give-way behaviour is activated. The give-way behaviour is realized by two forces, i.e. a lateral force to push the ego vehicle to the right adjacent lane, and a longitudinal force to pull the ego vehicle to slow down. Finally, if a CAV is selected as a CAV platoon member and it follows another CAV with the same platoon or the same class in the desired sequence on the target lane, it will degrade to the car-following mode by implementing only $p_{x,ij}^b$ with the front vehicle.

When the front vehicle drives with the maximum velocity and its gap with the following vehicle is larger than the equilibrium distance, the maximum velocity of the following vehicle is set to $v_x^{\max} + v_x^{\text{catch}}$ until the gap between them meets the equilibrium distance, where v_x^{catch} is a small positive value. This captures the approaching behaviour in the free traffic flow.

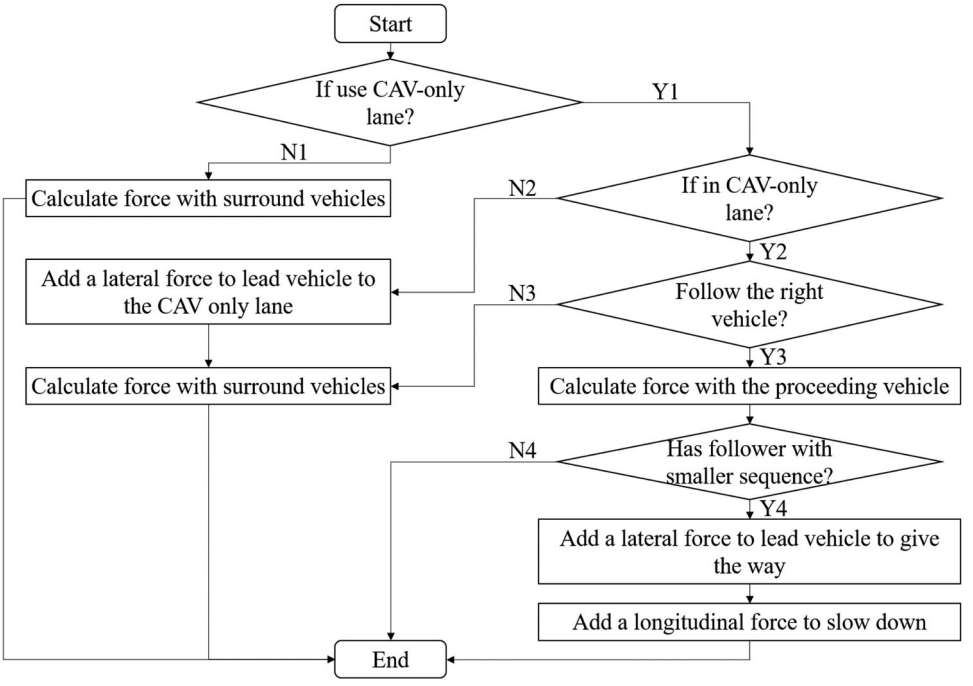

Figure 7. Work flow of the cooperative vehicle formation model.

In summary, the actions of vehicles are determined by the flow chart shown in Figure 7. The additional rules are also demonstrated in the flowchart. In the beginning, the first condition of whether the CAV uses the CAV-only lane is determined. If not (N1), the CAV is influenced by the inter-vehicle force and the cross-section force. If so (Y1), the second decision of whether the CAV is on the CAV-only lane is made. As to the second decision, an additional lateral force to change to the CAV-only lane is active if the condition is not satisfied (N2), and otherwise (Y2), the third decision of whether the CAV follows the vehicle as the controller asks is made. The operation of the third decision requires the calculation of either the inter-vehicle force with the front vehicle (Y3) or the force with surrounding vehicles (N3). The last decision of whether the follower possesses a smaller sequence is made after the third decision, and the path to Y4 activates the lateral additional rules of the lateral position and the sequence of its followers.

3. Mathematical model properties

This section provides a mathematical analysis of the proposed flock-like model. The rationality of the car-following behaviour is discussed in subsection 3.1. And then Section 3.2 proves the safety of the proposed flock-like model.

3.1. Car-following model analysis

This section aims to discuss the rationality of the car-following behaviour of the proposed model. In Wilson and Ward (2011), the plausible behaviour for general car-following models in the form of $a_{x,j} = f(\Delta x_j, \Delta v_{x,j}, v_{x,j})$ should have three properties as follows:

$$\frac{\partial a_{x,j}}{\partial \Delta x_j} > 0, \tag{13}$$

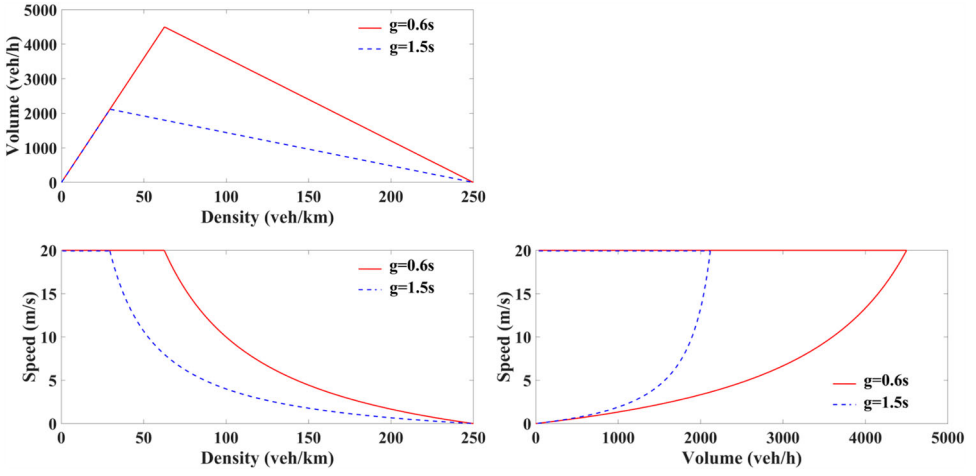

Figure 8. Fundamental diagram of the cooperative vehicle formation model. (L = 4 m, v_f = 20 m/s.)

$$\frac{\partial a_{x,j}}{\partial \Delta v_{x,j}} > 0, \tag{14}$$

$$\frac{\partial a_{x,j}}{\partial v_{x,j}} < 0, \tag{15}$$

where Δx_j and $\Delta v_{x,j}$ are calculated as in Equations (16) and (17).

$$\Delta x_j = x_{j-1} - x_j, \tag{16}$$

$$\Delta v_{x,j} = v_{x,j-1} - v_{x,j}. \tag{17}$$

The longitudinal acceleration of vehicle j during platooning is determined by $p^b_{x,j(j-1)}$ and p^d_j, as shown in Equation (18). The rational properties are proved from Equations (19) to (21).

$$\begin{aligned} a_{x,j}(t) = {} & \frac{c_{(j-1)j}}{m} \\ & \times \left(\ln\left(\Delta x_j(t)\right) - \frac{(x_e + t_c v_{x,j}(t) - t_h \Delta v_{x,j}(t)) \ln(x_e + t_c v_{x,j}(t) - t_h \Delta v_{x,j}(t))}{\Delta x_j(t)} \right) \\ & + p^d_j(v_{x,j}), \end{aligned} \tag{18}$$

$$\frac{\partial a_{x,j}(t)}{\partial v_{x,j}(t)} = -\frac{c_{(j-1)j}(t_c + t_h)}{m \Delta x_j(t)} (\ln(x_e + t_c v_{x,j}(t) - t_h \Delta v_{x,j}(t)) + 1) - \frac{F_{\max}}{v_x^{\max}} < 0, \tag{19}$$

$$\frac{\partial a_{x,j}(t)}{\partial \Delta v_{x,j}(t)} = \frac{c_{(j-1)j} t_h}{m \Delta x_j(t)} (\ln(x_e + t_c v_{x,j}(t) - t_h \Delta v_{x,j}(t)) + 1) > 0, \tag{20}$$

$$\begin{aligned} \frac{\partial a_{x,j}(t)}{\partial \Delta x_j(t)} = {} & \frac{c_{(j-1)j}}{m \Delta x_j(t)} \\ & \times \left(1 + \frac{(x_e + t_c v_{x,j}(t) - t_h \Delta v_{x,j}(t)) ln(x_e + t_c v_{x,j}(t) - t_h \Delta v_{x,j}(t))}{\Delta x_j(t)} \right) > 0. \end{aligned} \tag{21}$$

3.2. Emergency stopping scenario analysis

This subsection investigates the safety behaviour of the model when platoon leader suddenly decelerates from the desired velocity to a full stop, which is one of the most common test scenarios for

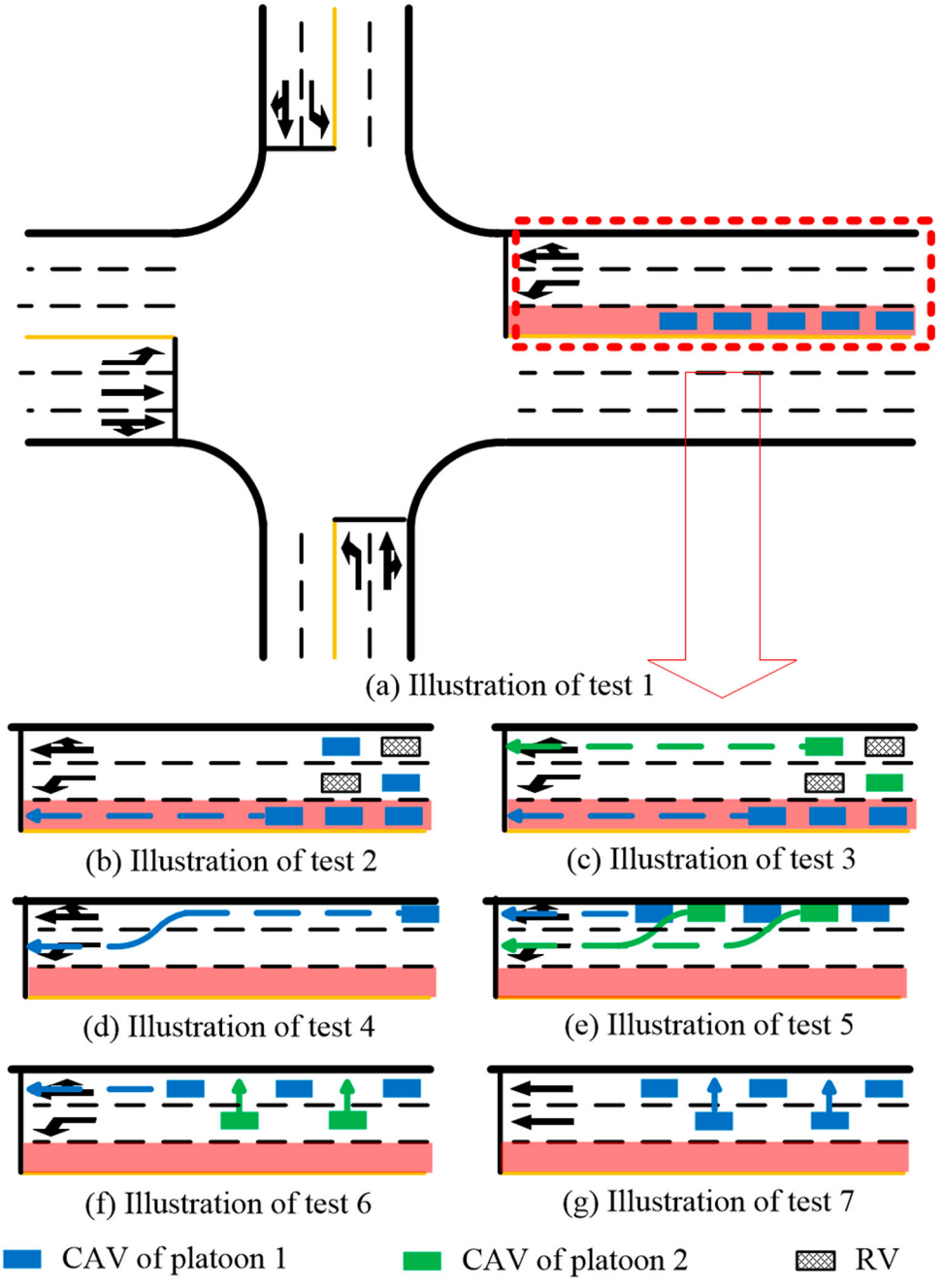

Figure 9. Illustration of test scenarios.

longitudinal safety. The emergency stropping process is analysed using discretization. The longitudinal distance can be calculated as follows.

$x_j(t)$ is a basic parameter in safety analysis, obtained by Equation (22). Equation (23) evolves from Equation (22). The special gap is a critical parameter for safety analysis, calculated using $x_{j-1}(t) - x_j(t)$,

as shown in Equation (24).

$$x_j(t) = x_j(0) + \Delta t \sum_{m=1}^{t-1} v_{x,j}(m) + \frac{\Delta t v_{x,j}(0)}{2} + \frac{\Delta t v_{x,j}(t)}{2}, \tag{22}$$

$$x_j(t) = x_j(0) + \Delta t \left(t v_{x,j}(0) + \sum_{m=0}^{t-1} \left(t - \frac{1}{2} - m \right) a_{x,j}(m) \right), \tag{23}$$

$$\frac{\Delta x_j(t)}{\Delta t} = \frac{x_e}{\Delta t} + \sum_{m=0}^{t-1} \left(t - \frac{1}{2} - m \right) (a_{x,j-1}(m) - a_{x,j}(m)). \tag{24}$$

By introducing $\Delta x_j(t-1)$ to Equation (24), the relationship between $\Delta x_j(t)$ and $\Delta x_j(t-1)$ is shown as in Equation (25).

$$\frac{\Delta x_j(t+1) - \Delta x_j(t)}{\Delta t} = \Delta t \sum_{m=0}^{t-1} (a_{x,j-1}(m) - a_{x,j}(m)) + \frac{\Delta t}{2} (a_{x,j-1}(t) - a_{x,j}(t)). \tag{25}$$

Since $v_{x,j-1}(0) = v_{x,j}(0)$, the first part of the left side, $\Delta t \sum_{m=0}^{t-1} (a_{x,j-1}(m) - a_{x,j}(m))$, is the velocity gap at time $t-1$. Equation (25) can be transformed into Equation (26).

$$\Delta x_j(t+1) - \Delta x_j(t) = \Delta v_{x,j}(t-1)\Delta t + \frac{\Delta t^2}{2} (a_{x,j-1}(t) - a_{x,j}(t)). \tag{26}$$

The relationship between the space headway when the vehicle has a full stop and the space headway at the initial state is shown in Equation (27), which is the summation of Equation (26) from $t = 0$ to $t = t_j^{\text{end}}$. t_j^{end} indicates the time when vehicle j has a full stop.

$$x_e - \Delta x_j(t_j^{\text{end}}) = \sum_{m=1}^{t_j^{\text{end}}} \Delta v_{x,j}(m) \Delta t. \tag{27}$$

With respect to the car-following behaviour, it is dangerous if a vehicle has to slow down with the largest allowable deceleration to avoid collision. Under this situation, the space headway when the vehicle has to fully stop can be indicated as

$$x_e - \Delta x_j(t_j^{\text{end}}) < \Delta v_x^{\max} \frac{v_x^{\max}}{a_x^{\min}}. \tag{28}$$

The space headway of the final state, $\Delta x_i^{t_j^{\text{end}}}$, needs to be larger than 0 to guarantee safety, therefore,

$$x_e > \Delta v_x^{\max} \frac{v_x^{\max}}{a_x^{\min}}. \tag{29}$$

In the initial state, all vehicles are operated at the desired velocity with the space headway of x_e. Then, the front vehicles start to slow down with the largest deceleration, while the following vehicles still travel with the desired velocity, until the space headway reaches the threshold $(p_{x,ij}^b)^{-1}(a_x^{\min})$. $(p_{x,ij}^b)^{-1}(a)$ is the reverse function of $p_{x,ij}^b$ with $\Delta v_{x,ij} = 0$. $(p_{x,ij}^b)^{-1}(a_x^{\min})$ is the space headway that leads to the largest deceleration. And the absolute value of the velocity gap $\Delta v_{x,ij}$ meets the maximum value

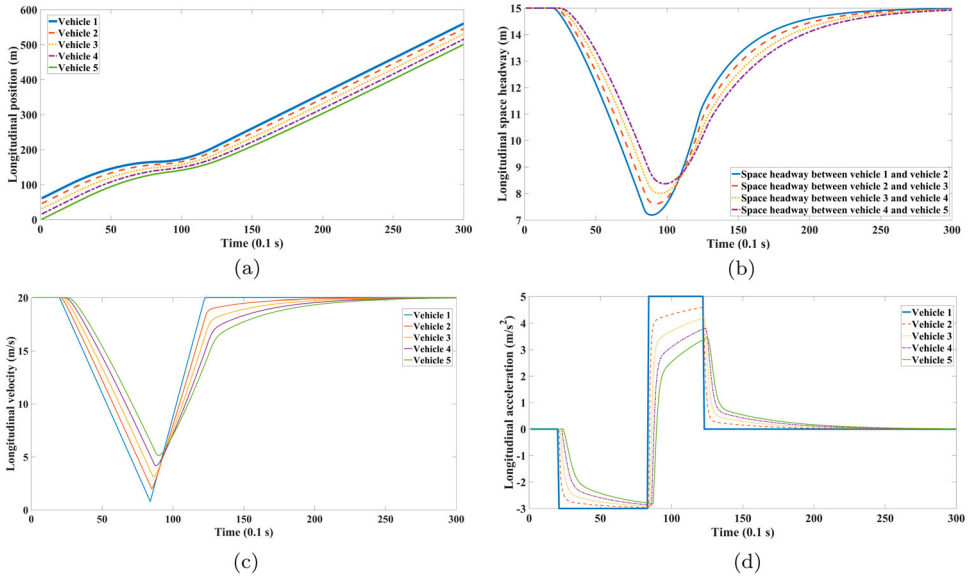

Figure 10. Result with x_e equals to 3. (a) Vehicle trajectories, (b) space headway-t figure, (c) longitudinal velocities figure, and (d) longitudinal accelerations figure.

when the space headway meet $(p^b_{x,ij})^{-1}(a^{\min}_x)$. The behaviours are illustrated in Equations (30) and (31).

$$\Delta v^{\max}_x = a^{\min}_x t_{\text{con}}, \tag{30}$$

where t_{con} indicates the time period of vehicle j driving at the constant largest velocity $v^{\max}_x$ after the deceleration of the front vehicle i.

$$\frac{a^{\min}_x {t_{\text{con}}}^2}{2} = (p^b_{x,ij})^{-1}(a^{\min}_x) - x_e. \tag{31}$$

According to Equations (30) and (31), $\Delta v^{\max}_x$ can be indicated as

$$\Delta v^{\max}_x = \sqrt{2a^{\min}_x((p^b_{x,ij})^{-1}(a^{\min}_x) - x_e)}. \tag{32}$$

By introducing Equations (29)–(32), the safety condition can be expressed as

$$x_e > v^{\max}_x \sqrt{\frac{2((p^b_{x,ij})^{-1}(a^{\min}_x) - x_e)}{a^{\min}_x}}. \tag{33}$$

If this condition of Equation (33) is respected, the platoon safety can be guaranteed under the scenario that the leader has a sharp deceleration from the desired velocity to a full stop. The space headway is always larger than a positive number, which is further proved in the following numerical experiments, as shown in Figures 10 and 11. The TTC of two vehicles in the same lane is defined as $\frac{\Delta x}{v_j - v_{j-1}}$. In the above two tests, TTC of different vehicles are shown in Figures 10 and 11. TTC are always larger than 5 and 15 s, respectively, in these two tests.

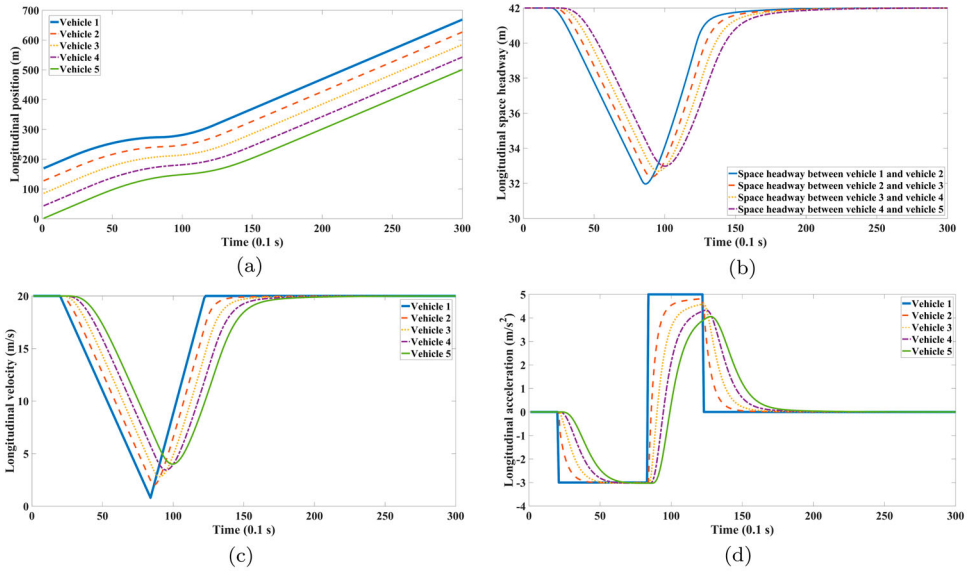

Figure 11. Result with x_e equals to 30. (a) Vehicle trajectories, (b) space headway-t figure, (c) longitudinal velocities figure, and (d) longitudinal accelerations figure.

3.3. String stability analysis

According to Ward (2009), the string stability can be proved by the following condition:

$$\left(\frac{\partial a_{x,j}(t)}{\partial v_{x,j}(t)}\right)^2 - \frac{\partial a_{x,j}(t)}{\partial \Delta x_j(t)} - \frac{\partial a_{x,j}(t)}{\partial v_{x,j}(t)}\frac{\partial a_{x,j}(t)}{\partial \Delta x_j(t)} > 0. \tag{34}$$

To simplify the notation, we define: $u = x_e + t_c v_{x,j}(t) - t_h \Delta v_{x,j}(t)$, and $k = \frac{(t_c+t_h)*c_{(j-1)j}}{m\Delta x_j(t)}$. Equation (34) is simplified using u and k, as following

$$\begin{aligned}\left(\frac{\partial a_{x,j}(t)}{\partial v_{x,j}(t)}\right)^2 - \frac{\partial a_{x,j}(t)}{\partial \Delta x_j(t)} - \frac{\partial a_{x,j}(t)}{\partial v_{x,j}(t)}\frac{\partial a_{x,j}(t)}{\partial \Delta x_j(t)} &= k^2\ln(u)^2 + \left(k(k-1) + \frac{F_{\max}k}{v_x^{\max}}\right)u\ln(u) \\ &+ \frac{k(k-1)u\ln(u) + k^2u\ln(u)^2}{\Delta x_j(t)} \\ &+ \left(3k^2 + \frac{2F_{\max}k}{v_x^{\max}}\right)\ln(u) + 5k^2 - k. \end{aligned} \tag{35}$$

Equation (35) is larger than 0 when $u > 1$ and $k > 1$. $u > 1$ implies the following:

$$v_{x,j-1}(t) < v_{x,j}(t) + \frac{t_d v_{x,j}(t) + x_e - 1}{t_h}. \tag{36}$$

This condition can be easily met. Assuming a platoon with the velocity of 10 m/s, and t_c and t_h are set as 0.6 s, x_e is 10 m. This condition can only be violated if the vehicle in front is faster 25 m/s at least than the following vehicle, which is essentially not a platoon anymore.

$k > 1$ is ensured when $c_{(j-1)j}$ is large enough, that is,

$$c_{(j-1)j} > \frac{\Delta x_j(t)}{t_h + t_c}. \tag{37}$$

The string stability is guaranteed the conditions of Equations (36) and (37) are met. As in Figure 10, the first vehicle has a small disturbance, and the fluctuation is convergent.

3.4. Traffic flow characteristics

The traffic flow characteristics are important for applying the proposed cooperative vehicle formation model. We can analytically derive the fundamental diagram of CACC traffic flow, which is of triangular shape (Zhang et al. 2020). The basic values in the triangular fundamental diagram of the constant time gap CACC model are listed as follows:

$$k_c = \frac{1000}{gv_f + L}, \tag{38}$$

$$q_c = \frac{3600}{g + L/v_f}, \tag{39}$$

$$k_j = \frac{1000}{L}, \tag{40}$$

where k_c is the capacity density, q_c is the capacity, k_j is the jam density, v_f is free speed, g is the time headway, and L is the length of vehicle. According to the above parameters, the fundamental diagram is shown in Figure 8. With an increase in density, the flow increases linearly. With $g = 0.6$ s, the capacity flow, which is 4500 pcu/h, is reached at the critical density k_c, and a higher time headway lead a lower capacity and a lower critical density k_c, as shown in Figure 8. The space-mean between origin and k_c is stable as v_f. However, after the density exceeding k_c, the volume starts to drop as a curve. And when the density meets k_j, the volume drops to 0. The speed for any point on the curve is defined as the slope of the line through that point and the origin. Therefore, the traffic flow characteristics of the proposed cooperative vehicle formation model comply with the traffic flow theory. To apply the proposed model at a signalized intersection, the saturation flow should be calculated first using the base saturation flow rate and relative adjustment factors (Board 2010). In this proposed algorithm, the saturation flow rate of the CAV-only lane at an intersection is 4500 pcu/h, which is higher than the realistic saturation flow (normally less than 2000 pcu/h/lane (Board 2010)).

4. Numerical experiments

In this section, numerical experiments are conducted to demonstrate the workings of the proposed flock-like model. The experiments are designed in Section 4.1. Then, the experimental results are presented in Section 4.2, followed by the discussions and conclusions on the experimental results in Section 4.3.

4.1. Experimental design

The numerical experiments aim to verify the behaviours of the proposed flock-like model. The scenarios are designed to demonstrate the typical behaviours of car following, lane changing, platooning and splitting, which can be accordingly categorized into longitudinal scenarios, two-dimensional scenarios and comprehensive scenarios. The longitudinal scenario aims to evaluate the car-following behaviour within a platoon (see Platoon emergency stopping test in Table 1). The two-dimensional scenarios are proposed to verify the lane changing, splitting and platoon forming behaviours for an individual vehicle and further for multiple vehicles (see Single platoon forming test, Multi-platoons forming test, Single vehicle lane changing test, and Multi-vehicles separation test in Table 1). The comprehensive scenarios test the performance of forming a single platoon and multiple platoons under the mixed traffic environment (see Vehicles not in a group form in a platoon test and Vehicles in a group form in a platoon test in Table 1).

All test scenarios are illustrated in Figure 9. The pink lane in this figure is the CAV dedicated lane, and vehicles in a same platoon have the same colour. The length of the test road is set as 600 m with the link velocity limitation of 20 m/s. An intersection is located on the link at the longitudinal position of 400 m. The numerical study is simulated in MATLAB platform for a period of 30 s.

Table 1. Numerical experimental design.

Test number	Class	Scenario	Purpose
1	Longitudinal Scenario	Platoon emergency stopping	Car following in accelerating and decelerating
2	Comprehensive Scenario	Single platoon forming	Cooperative merging
3	Comprehensive Scenario	Multi-platoons forming	Management and cooperative merging
4	Comprehensive Scenario	Low penetration platoons forming	Influence of HVs
5	Two-dimensional Scenario	Single vehicle lane changing	Lane changing with different values of parameters
6	Two-dimensional Scenario	Multi-vehicles separation	Lane changing and platoon separation with different values of parameters
7	Two-dimensional Scenario	Vehicles not in a group form in a platoon	Lane changing and platoon forming with different values of parameters
8	Two-dimensional Scenario	Vehicles in a group form in a platoon	Lane changing and platoon forming with different values of parameters

In the numerical experiments, the maximum longitudinal acceleration, the maximum longitudinal deceleration, the maximum lateral acceleration, the maximum longitudinal velocity and the maximum lateral velocity are set to be 3, -5, 2 m/s^2, 20 and 1 m/s, respectively.

4.2. Numerical experimental result

For all tests, the model can run in real-time. In the Platoon emergency stopping test, the car-following behaviour is shown to be safe by using the 'emergency stopping' scenario, as shown in Figure 10. A platoon composed of five CAVs is proposed to test this scenario. At first, all vehicles travel with the desired velocity, and the distances between each pair of adjacent vehicles are equal to the equilibrium distance. The first vehicle has an emergency brake at around 20 s and decelerates until 0 m/s, and then it accelerates to the maximum velocity again, as shown in the V-t subfigure in Figure 10. According to the safety analysis discussed in Equation (33), safety can be guaranteed if the equilibrium distance is larger than a threshold value. Different parameter values of $x_e = 3$ m and $x_e = 30$ m are tested, respectively, and the corresponding trajectories, space headway, velocity and acceleration of vehicles in the platoon under $x_e = 3$ m and $x_e = 30$ m are presented in Figures 10 and 11. All vehicles respect the safe driving requirements, although the minimum gap is smaller than the propagation of the platoon and the velocity fluctuations are amplified. However, in the space headway-t subfigures of Figures 10 and 11, the minimum gap is finally stable at around 1 and 10 m, respectively, in spite of the fluctuating platoon propagation, which proves the conclusion of Section 3.2 that the final longitudinal gap will always be larger than a value. And this value can be adjusted by using suitable parameters such as x_e. Additionally, by comparing Figures 10 and 11, it can be found that larger values of x_e also lead to larger minimum space headways, while lower values of x_e result in faster convergence.

Hereinafter, the experiments of three scenarios are demonstrated under the mixed traffic environment. The platoon forming under a high CAV penetration environment is tested in the first two scenarios, i.e. the single platoon scenario (Single platoon forming test) and the multi-platoon scenario (Multi-platoons forming test). Seven vehicles composed of five CAVs and two HVs are initially set on different lanes of the test link. In the first experiment, the five CAVs form a platoon from different lanes. The desired velocity of all vehicles is 20 m/s. The longitudinal and lateral trajectories are shown in Figure 12. It is clear that the vehicle sequence is adjusted in this figure, e.g. vehicles 4 and 5 take over vehicles 2 and 3. Providing CAV exclusive lanes, this performance is beneficial to the improvement in lane utilization under the adaptive control at the urban network. The proposed model can complete the platoon sequence adjustment around 90 m and the platoon formation around 150 m to the adjusting-start-line.

The multi-platoon scenario is tested considering two platoons. Platoon 1 is composed of vehicle 1, 4 and 5, and platoon 2 consists of vehicles 2 and 3. Vehicles 1 and 2 are the leader of platoon 1 and

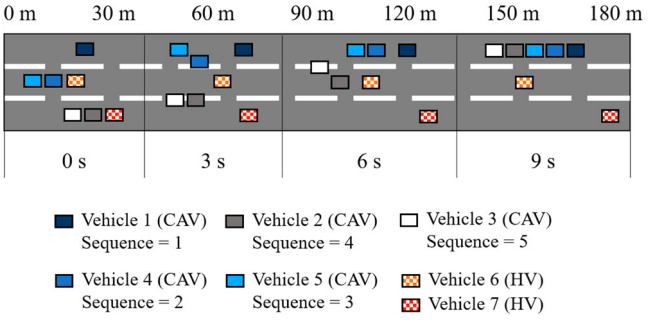

Figure 12. Test result of Single platoon forming test.

platoon 2, respectively. The desired velocity of platoon 1 is set to 20 m/s, while the desired velocity of platoon 2 is 18 m/s. More than four-lane changing and overtaking behaviours are applied to form platoons. The results of the multi-platoon scenario are shown in Figure 13. The platoon formation finishes within 150 m. HVs keep the initial driving strategy because they are not influenced by the following CAVs. If CAVs form platoons passively without lane changing (for instance, forming platoons according to the communication range, which is widely used in the existing platoon-based urban traffic control models (Cooper et al. 2016; Jin et al. 2013)), three platoons are generated, respectively, on their initial lanes, i.e. vehicle 1, vehicles 3 and 5, and vehicles 2 and 4. In this way, vehicles 4 and 5 cannot reach the desired velocity, and even no platoon is formed if they have different routes. On the other hand, if CAVs form platoons passively with considering lane changing, there are still three platoons, that is, vehicle 1, vehicles 2 and 3, and vehicles 4 and 5. Since vehicle 2 and vehicle 4 are in the same lane, the platoon composed of vehicles 4 and 5 has to follow platoon 2. Vehicle 4 and vehicle 5 cannot reach the desired velocity. If they have different routes, vehicle 4 and vehicle 5 possibly have to wait for another signal cycle to pass the intersection, causing additional travel delay. Through the Single platoon forming test and Multi-platoons forming test, the proposed flock-like model can incorporate the vehicle sequence adjustment and the reasonable two-dimensional motions, both of which are able to better utilize the urban temporal-spatial resource under the adaptive control at intersections. To conclude, the proposed flock-like model has a good performance in the numerical experiments.

In addition, a scenario under a low CAV penetration rate is also tested. The vehicle composition is 5 HVs and 2 CAVs. The test results are shown in Figure 14. The simulation demonstrates that CAVs can form platoons in a short time (around 10 s) in a low penetration rate.

4.3. Discussion

In this section, an analysis of several numerical experiments is discussed. As mentioned above, the Platoon emergency stopping test shows that the platoon safety can be guaranteed, and the Single platoon forming test and Multi-platoons forming test show the value of the proposed algorithm. However, there are several parameters that may influence the performance of the proposed algorithm. The reasonable parameter ranges still need to be explored. Several two-dimensional scenarios, including individual vehicle scenarios and multi-vehicle scenarios, are proposed to explore it (Single vehicle lane changing test, Multi-vehicles separation test, Vehicles not in a group form in a platoon test, and Vehicles in a group form in a platoon test). The objective of the single-vehicle test (Single vehicle lane changing test) is to change to the target lane in the vicinity of intersection. The test vehicle is initially on the right lane, and intends to use the left lane to pass the intersection under appropriate parameter values. Two-dimensional scenarios of multi-vehicle tests are designed to validate platoon forming and splitting at the intersection, including vehicles from different platoon numbers splitting after passing the intersection (Multi-vehicles separation test); vehicles from different platoon numbers forming a platoon before passing the intersection (Vehicles not in a group form in a platoon test); and vehicles

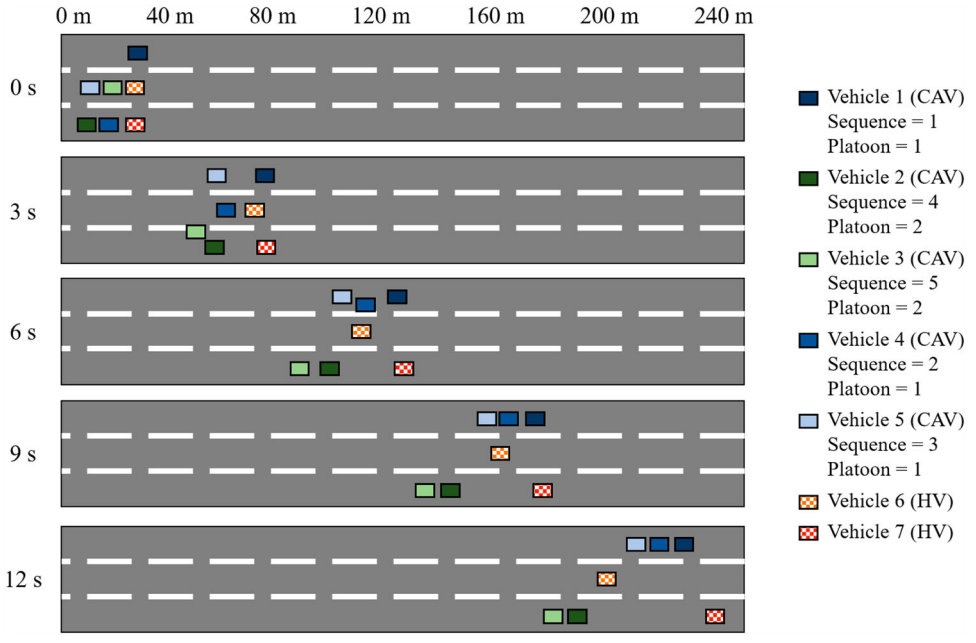

Figure 13. Test result of multi-platoons forming test.

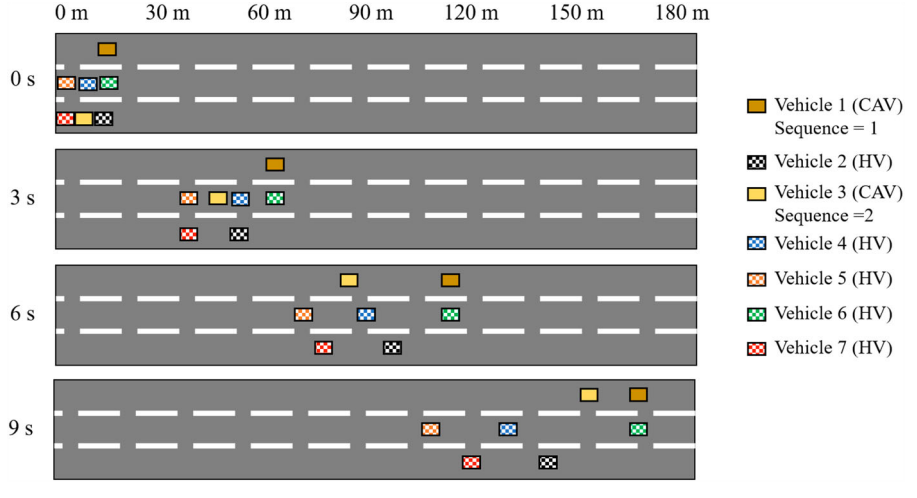

Figure 14. Test result of low penetration platoons forming test.

from the same platoon number forming a platoon at the link (Vehicles in a group form in a platoon test). Parameters such as height h, friction f and attraction strength c_{ij} will influence the above-mentioned scenarios. For scenarios considering vehicles from different platoon numbers (Multi-vehicles separation test and vehicles not in a group form in a platoon test), the platoon forming and splitting are dominated by p_j^c, which transforms these scenarios into the single-vehicle lateral scenario (Single vehicle lane changing test). As for vehicles in a group form in a platoon test, vehicles with the same number of platoon or class are required to form a platoon, and p_{ij}^b dominates the platoon formation. Thus, the critical parameter is the attraction strength c_{ij}. Single vehicle lane changing test, Multi-vehicles separation test, Vehicles not in a group form in a platoon test, and Vehicles in a group form in a platoon test

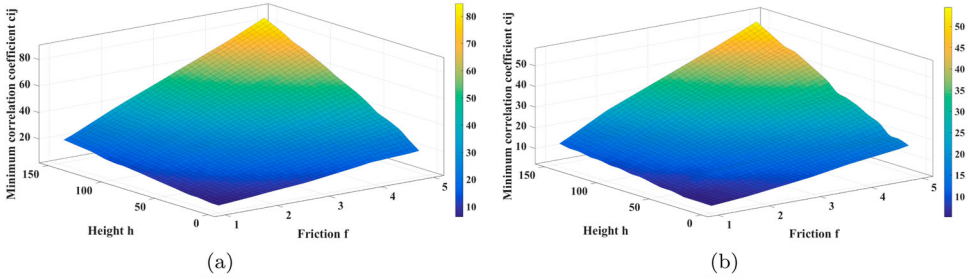

Figure 15. Reasonable range of minimum attraction strength. (a) Vehicles in adjacent lane and (b) vehicles separated by one lane.

show that the proposed model can generate reasonable behaviours under the reasonable parameter ranges. According to the Single vehicle lane changing test, Multi-vehicles separation test, and Vehicles not in a group form in a platoon test, both height h and friction f can influence the performance of the model, and the reasonable ranges are $h \in [110, 150]$ and $f \in [1, 4]$. As for Vehicles in a group form in a platoon test, the minimum attraction strength c_{ij} in the platoon forming scenario is explored under the reasonable ranges of h and f, as shown in Figure 15. Both the situation of vehicles locating on adjacent lanes and the situation that two vehicles are separated by one lane are tested. The minimum attraction strength c_{ij} increases with the growth of height h and friction f. Since larger vehicle gaps lead to larger attractions, the minimum attraction strength c_{ij} of vehicles in the adjacent lane is larger than the minimum attraction strength c_{ij} of vehicles separated by one lane with same values of height h and friction f, as shown in Figure 15. If vehicles are separated by more than one lane, the minimum attraction strength c_{ij} will be much smaller. Suitable value of the minimum attraction strength c_{ij} can be selected according to the number of lanes, height h and friction f.

5. Conclusion

This paper presents a flock-like two-dimensional model for cooperative vehicle groups. This model describes platoon formation process with flocking principles under the mixed traffic environment of CAVs and HVs. The model can be applied to situations where formation instructions are given by traffic controllers or as self-organizing processes based on vehicle classes. The potential filed theory is the basis of the model and some rules are added for better adapting to realistic scenarios. The potential field is composed of the inter-vehicle potential field and the cross-section potential field.

The mathematical properties of the model are examined. The car-following behaviour is shown to respect the rational car-following behaviour. The safety of the proposed model is also analysed and verified under an emergency braking scenario. Seven numerical experiments are designed to test the performance of the proposed model, and the reasonable ranges of parameters in the flock-like model are explored. In the longitudinal scenarios, the safety of CAV platoon is mainly considered and proved. As for the two-dimensional scenarios, the platoon formation and the split behaviours labelled with different platoon numbers or classes in the vicinity of the intersection are tested, in addition to the platoon formation behaviour of vehicles with the same platoon number or class. The simulation results show that the proposed model can mimic the platoon operation in a wide range of manoeuvres, including normal car-following, emergency braking, platoon merging and splitting in mixed traffic.

This paper explores platoon operations in the mixed traffic of CAVs and HVs. Further research is directed to integrate the traffic control algorithm with the proposed platoon dynamics model. The behaviours of human drivers and the trajectory planning of CAVs can be improved in the future. Additionally, the impact of the platoon formation model on traffic operations can be assessed in terms of capacity and safety.

Acknowledgments

The views presented in this paper are those of the authors alone.

Disclosure statement

No potential conflict of interest was reported by the author(s).

Funding

This research was funded by Shanghai Sailing Program [grant number 22YF1452600], the National Natural Science Foundation of China [grant numbers 52131204, 61903276, 51722809], and the Fok Ying Tong Education Foundation [grant number 151076].

ORCID

Wanjing Ma http://orcid.org/0000-0002-9403-3174
Bart van Arem http://orcid.org/0000-0001-8316-7794

References

Bang, S., and S. Ahn. 2017. "Platooning Strategy for Connected and Autonomous Vehicles: Transition from Light Traffic." *Transportation Research Record: Journal of the Transportation Research Board* 2623 (1): 73–81.

Baskar, L. D., B. De Schutter, J. Hellendoorn, and Z. Papp. 2011. "Traffic Control and Intelligent Vehicle Highway Systems: A Survey." *IET Intelligent Transport Systems* 5 (1): 38–52.

Board, T. R. 2010. *Highway Capacity Manual 2010*, 1207. Washington, DC: National Research Council.

Cao, Y., W. Yu, W. Ren, and G. Chen. 2012. "An Overview of Recent Progress in the Study of Distributed Multi-agent Coordination." *IEEE Transactions on Industrial Informatics* 9 (1): 427–438.

Chen, W., Y. Liu, X. Yang, Y. Bai, Y. Gao, and P. Li. 2015. "Platoon-Based Speed Control Algorithm for Ecodriving at Signalized Intersection." *Transportation Research Record: Journal of the Transportation Research Board* 2489 (1): 29–38.

Chen, N., M. Wang, T. Alkim, and B. van Arem. 2018. "A Robust Longitudinal Control Strategy of Platoons Under Model Uncertainties and Time Delays." *Journal of Advanced Transportation* 2018: 9852721.

Cooper, C., D. Franklin, M. Ros, F. Safaei, and M. Abolhasan. 2016. "A Comparative Survey of VANET Clustering Techniques." *IEEE Communications Surveys & Tutorials* 19 (1): 657–681.

Das, B., B. Subudhi, and B. B. Pati. 2016. "Cooperative Formation Control of Autonomous Underwater Vehicles: An Overview." *International Journal of Automation and Computing* 13 (3): 199–225.

Faraj, M., F. E. Sancar, and B. Fidan. 2017. "Platoon-based Autonomous Vehicle Speed Optimization Near Signalized Intersections." In *2017 IEEE Intelligent Vehicles Symposium (IV)*, 1299–1304. IEEE.

Hallé, S., J. Laumonier, and B. Chaib-Draa. 2004. "A Decentralized Approach to Collaborative Driving Coordination." In *Proceedings of the 7th International IEEE Conference on Intelligent Transportation Systems (IEEE Cat. No. 04TH8749)*, 453–458. IEEE.

Han, X., R. Ma, and H. M. Zhang. 2020. "Energy-aware Trajectory Optimization of CAV Platoons Through a Signalized Intersection." *Transportation Research Part C: Emerging Technologies* 118: 102652.

Jia, D., K. Lu, J. Wang, X. Zhang, and X. Shen. 2015. "A Survey on Platoon-based Vehicular Cyber-physical Systems." *IEEE Communications Surveys & Tutorials* 18 (1): 263–284.

Jia, D., D. Ngoduy, and H. L. Vu. 2019. "A Multiclass Microscopic Model for Heterogeneous Platoon with Vehicle-to-Vehicle Communication." *Transportmetrica B: Transport Dynamics* 7 (1): 311–335.

Jin, I. G., and G. Orosz. 2016. "Optimal Control of Connected Vehicle Systems with Communication Delay and Driver Reaction Time." *IEEE Transactions on Intelligent Transportation Systems* 18 (8): 2056–2070.

Jin, Q., G. Wu, K. Boriboonsomsin, and M. Barth. 2013. "Platoon-based Multi-agent Intersection Management for Connected Vehicle." In *16th International IEEE Conference on Intelligent Transportation Systems (ITSC 2013)*, 1462–1467. IEEE.

Kanagaraj, V., and M. Treiber. 2018. "Self-driven Particle Model for Mixed Traffic and Other Disordered Flows." *Physica A: Statistical Mechanics and its Applications* 509: 1–11.

Li, Y., W. Chen, S. Peeta, X. He, T. Zheng, and H. Feng. 2017. "An Extended Microscopic Traffic Flow Model Based on the Spring-mass System Theory." *Modern Physics Letters B* 31 (09): 1750090.

Li, Z., F. Khasawneh, X. Yin, A. Li, and Z. Song. 2019. "A New Microscopic Traffic Model Using a Spring-Mass-Damper-Clutch System." *IEEE Transactions on Intelligent Transportation Systems* 21: 3322–3331.

Luo, F., J. Larson, and T. Munson. 2018. "Coordinated Platooning with Multiple Speeds." *Transportation Research Part C: Emerging Technologies* 90: 213–225.

Otto, J. S., and F. E. Bustamante. 2009. "Distributed or Centralized Traffic Advisory Systems: The Application's Take." In *2009 6th Annual IEEE Communications Society Conference on Sensor, Mesh and Ad Hoc Communications and Networks*, 1–10. IEEE.

Pei, H., S. Feng, Y. Zhang, and D. Yao. 2019. "A Cooperative Driving Strategy for Merging at On-Ramps Based on Dynamic Programming." *IEEE Transactions on Vehicular Technology* 68: 11646–11656.

Ren, W., and Y. Cao. 2010. *Distributed Coordination of Multi-agent Networks: Emergent Problems, Models, and Issues*. London, Springer Science & Business Media.

Reynolds, C. W. 1987. "Flocks, Herds and Schools: A Distributed Behavioral Model." In *Proceedings of the 14th Annual Conference on Computer Graphics and Interactive Techniques, SIGGRAPH '87*, 25–34. New York, NY: Association for Computing Machinery.

Rios-Torres, J., and A. A. Malikopoulos. 2016. "A Survey on the Coordination of Connected and Automated Vehicles at Intersections and Merging at Highway On-Ramps." *IEEE Transactions on Intelligent Transportation Systems* 18 (5): 1066–1077.

Sau, J., J. Monteil, and M. Bouroche. 2019. "State-Space Linear Stability Analysis of Platoons of Cooperative Vehicles." *Transportmetrica B: Transport Dynamics* 7 (1): 18–43.

Shladover, S. E., C. Nowakowski, X. Y. Lu, and R. Ferlis. 2016. "Cooperative Adaptive Cruise Control: Definitions and Operating Concepts." *Transportation Research Record Journal of the Transportation Research Board* 2489: 145–152.

Tallapragada, P., and J. Cortés. 2017. "Distributed Control of Vehicle Strings Under Finite-time and Safety Specifications." *IEEE Transactions on Control of Network Systems* 5 (3): 1399–1411.

Tan, H.-S., R. Rajamani, and W.-B. Zhang. 1998. "Demonstration of an Automated Highway Platoon System." In *Proceedings of the 1998 American control conference. ACC (IEEE Cat. No. 98CH36207)*, Vol. 3, 1823–1827. IEEE.

Turri, V., B. Besselink, and K. H. Johansson. 2016. "Cooperative Look-ahead Control for Fuel-efficient and Safe Heavy-duty Vehicle Platooning." *IEEE Transactions on Control Systems Technology* 25 (1): 12–28.

Van de Hoef, S. 2016. "Fuel-efficient Centralized Coordination of Truck Platooning." PhD thesis, KTH Royal Institute of Technology.

Wang, M., W. Daamen, S. P. Hoogendoorn, and B. van Arem. 2014. "Rolling Horizon Control Framework for Driver Assistance Systems. Part II: Cooperative Sensing and Cooperative Control." *Transportation Research Part C: Emerging Technologies* 40: 290–311.

Wang, Z., G. Wu, and M. J. Barth. 2018. "A Review on Cooperative Adaptive Cruise Control (CACC) Systems: Architectures, Controls, and Applications." In *2018 21st International Conference on Intelligent Transportation Systems (ITSC)*, 2884–2891. IEEE.

Ward, J. A. 2009. "Heterogeneity, Lane-changing, Instability in Traffic: A Mathematical Approach." PhD thesis, University of Bristol.

Wilson, R. E., and J. A. Ward. 2011. "Car-following Models: Fifty Years of Linear Stability Analysis: A Mathematical Perspective." *Transportation Planning and Technology* 34 (1): 3–18.

Yao, S., R. A. Shet, and B. Friedrich. 2020. "Managing Connected Automated Vehicles in Mixed Traffic Considering Communication Reliability: A Platooning Strategy." *Transportation Research Procedia* 47: 43–50.

Yi, Z., L. Li, X. Qu, Y. Hong, P. Mao, and B. Ran. 2020. "Using Artificial Potential Field Theory for a Cooperative Control Model in a Connected and Automated Vehicles Environment." *Transportation Research Record: Journal of the Transportation Research Board* 2674 (9): 1005–1018.

Zhan, Z., S. M. Wang, T. L. Pan, P. Chen, W. H. K. Lam, R. X. Zhong, and Y. Han. 2021. "Stabilizing Vehicular Platoons Mixed with Regular Human-piloted Vehicles: An Input-to-State String Stability Approach." *Transportmetrica B: Transport Dynamics* 9 (1): 569–594.

Zhang, Y., Y. Bai, J. Hu, and M. Wang. 2020. "Control Design, Stability Analysis, and Traffic Flow Implications for Cooperative Adaptive Cruise Control Systems with Compensation of Communication Delay." *Transportation Research Record: Journal of the Transportation Research Board* 2674 (8): 638–652.